Enzymatic Assay in a Lab-on-a-Disk Format to Measure Free Piperacillin Concentration in Serum

Olivier Verlaine[1,2], Ana Amoroso[2], Maxence Remy[3], Stéphanie Wautier[3], Raphaël Robiette[3], Bernard Joris[2], Tristan Gilet[1*]

[1]Microfluidics Lab, Department of Aerospace and Mechanical Engineering, University of Liège, Allée de la Découverte, 13, 4000 Liège, Belgium.
[2]Center for Protein Engineering, InBIOS, Department of Life Sciences, University of Liège, Allée du 6 Août, 13, 4000 Liège, Belgium.
[3]Institute of Condensed Matter and Nanosciences, Université Catholique de Louvain, Place Louis Pasteur 1, bte L4.01.06, 1348, Louvain-la-Neuve, Belgium.

*Corresponding author(s). E-mail(s): Tristan.Gilet@uliege.be;

Abstract

This work describes a method based on an enzymatic assay to measure the free concentration of piperacillin (a β-lactam antibiotics) in blood serum. The assay is based on the release of fluorescent umbelliferone, upon hydrolysis by BlaP99 β-lactamase of a substrate in competition with piperacillin. The assay is implemented in a lab-on-a-disk (LoaD) setup, in which samples and reagents are manipulated with robust centrifugal microfluidic techniques. To encounter the needs and constraints of Therapeutic Drug Monitoring (TDM) at bedside, the system is entirely automated and miniaturized. Within a few minutes and from a few microliters of serum, it provides piperacillin concentration measurements in a clinically meaningful range. This paper describes the design and characterization of the chemical kinetics and the microfluidic strategy underlying this assay. The data are compared to measurements made in well-plates with a conventional method.

Keywords: Centrifugal microfluidics, antibiotic dosage, therapeutic drug monitoring, enzymatic assay

1 Introduction

β-lactam antibiotics are amongst the most prescribed drugs in clinical setting. They proved broad antibacterial spectrum, efficacy and relatively low incidence of adverse events [1]. They are classified as time-dependent killers, meaning their effectiveness is primarily determined by the time during which their concentration exceeds the Minimum Inhibitory Concentration (MIC). Further increase in concentration does not provide more rapid or more efficient killing against most pathogens [2]. Notably, only the free, unbound portion of the antibiotic – the one not bound to proteins – contributes to this activity. Most β-lactams exhibit protein binding, predominantly to serum albumin, often in a linear, dose-proportional way that depends on the antibiotic (e.g., 2% meropenem, up to 98% for ceftriaxone). Consequently, when β-lactam concentrations are reported, they must be adjusted for protein binding to estimate free exposure [3].

β-lactam antibiotics are widely utilized across diverse patient populations. Despite the variability in patient characteristics and illness, these drugs are frequently administered using fixed dosing regimens based on studies of healthy adult volunteers. However, a deeper understanding of pharmacokinetics/pharmacodynamics (PK/PD) principles specifically related to antibiotics reveals significant inter-patient variability in drug exposure necessary for an effective killing of bacterial cells. This highlights the potential benefits of personalized dosing strategies to improve clinical response. Therapeutic Drug Monitoring (TDM) has traditionally targeted drugs with narrow therapeutic window in which toxicity had to be prevented. More recent approaches aim to improve therapeutic results and maximize positive clinical outcomes [3, 4]. In acute care patients with multi-organ dysfunction, obesity and/or advanced age, the PK/PD profiles are highly unpredictable. In these group cases, TDM for β-lactam antibiotics facilitates precision dosing by accommodating individual patient characteristics [5]. This strategy not only aims to prevent treatment failure and toxicity but also helps mitigate the emergence of resistance.

Effective implementation of β-lactam TDM relies on accurately assessing the free antibiotic blood levels. The most common in-house methods for β-lactam quantification involve reverse phase high performance liquid chromatography (RP-HPLC) coupled with ultraviolet (UV) or tandem mass spectrometric (MS-MS) detection. These methods require specific costly instruments operated by trained personnel. To ensure rapid result availability, these instruments must be kept in standby, limiting their use for other analyses. Due to their complexity, they are typically housed in specialized laboratories, which hinders real-time interaction with healthcare professionals managing individual patients. Additionally, the instability of β-lactams at room temperature presents pre-analytical challenges. Consequently, samples must be kept on ice or frozen until being processed to minimize (though not entirely prevent) degradation. Timely availability of concentration results is crucial for effective dose optimization. Indeed, delays can render the results clinically irrelevant, particularly in patients undergoing rapid physiological and interventional changes [6–10]. Therefore, the absence of approved assays for in-situ testing of β-lactam concentrations poses a

significant barrier to broader TDM accessibility [6, 7]. It reduces the number of institutions capable of offering TDM for β-lactams due to financial (high investment and maintenance costs) and practical limitations.

A method of quantification of β-lactam antibiotics was developed with the aim to address the challenges of TDM [11, 12]. This approach is based on the hydrolysis of a chromogenic reporter substrate by an enzyme, specifically a β-lactamase. The concentration of the product of this hydrolysis is monitored over time. The β-lactam antibiotic serves as a competitive inhibitor: the catalytic activity of the enzyme becomes distributed between the reporter substrate and the antibiotic, so the rate of production of the monitored product decreases in presence of the antibiotic. By measuring this apparent loss of enzymatic activity, the concentration of free (non-protein-bound) β-lactams in serum can be accurately determined in real time. The corresponding reactions and kinetic equations are developed in the supplementary material. For initial enzyme, antibiotic and substrate concentrations denoted e_0, a_0 and s_0 respectively, the resulting production rate v of hydrolyzed substrate is given by

$$v = \frac{k_{\text{cat}} e_0 s_0}{s_0 + K_{\text{m}} + \frac{K_{\text{m}}}{K'_{\text{m}}} a_0}, \tag{1}$$

where K_{m} and K'_{m} are the Michaelis constants associated to the β-lactamase of the substrate and the antibiotic, respectively, and k_{cat} is the catalytic rate constant of the substrate. The antibiotic concentration is found as

$$a_0 = \gamma \left(\frac{v_{\max}}{v} - 1 \right), \qquad \gamma = K'_{\text{m}} \left(1 + \frac{s_0}{K_{\text{m}}} \right), \tag{2}$$

where $v_{\max}$ is the rate of hydrolysis in absence of antibiotic. A possible choice for the enzyme is BlaP99, namely a class C β-lactamase biosensor from *Enterobacter cloacae*. This enzyme enables the quantitative, real-time measurement of free β-lactam concentrations in serum samples within a microbiologically, therapeutically, and toxicologically meaningful range, e.g., from 2 to 1000 mg/L for piperacillin (i.e., approximately from 4 μM to 2 mM). Details on the validation of the piperacillin assay are provided in the Supplementary Material (Section 4). They are also available in [11], together with a non-exhaustive list of β-lactam antibiotics (including carbapenems) that can be quantified using the BlaP99 β-lactamase. Importantly, BlaP99 is highly specific, so inherently insensitive to non-β-lactam drugs. It minimizes potential interference from other medications or endogenous substances present in critically ill patients.

To be used in a TDM configuration, this method must be implemented in a fully-automated Point-of-Care (PoC) device. Transport of the sample to an external laboratory should be avoided, and the turn-around time must be less than an hour. The method must also be adapted to handle less than 10 μL of serum if it is to be used on infants. The Lab-on-a-Disk (LoaD) technology allows such automation and miniaturization. It consists in handling defined volumes (of the order of microliters) of liquid samples and reagents through a network of microfluidic channels and chambers engraved in a disk. The spinning speed of this disk is varied to provide the

requested centrifugal force and control fluid flows therein [13, 14]. Defined volumes of reagents can be selected (metering) thanks to an overflow principle [15]. Many strategies have been proposed to complement this control, including a wealth of different valve mechanisms [16, 17].

Duffy et al. [18] reported the design of a LoaD to conduct a similar enzymatic assay, for which the prototype can possibly be turned to a point-of-care instrument. However, this LoaD has three shortcomings that prevent its direct adaptation to β-lactam TDM. First, the read-out is an absorbance rate measurement sensitive in the range $[1, 10]$ mM. This is several orders of magnitude higher than what should be targeted for β-lactam TDM. The optical length is limited by the thickness of the spinning disk, so it cannot be increased by several orders of magnitude. Consequently, the relevant range of β-lactam concentration of TDM seems out of reach to an absorbance measurement across the thickness of a microfluidic disk. The second shortcoming is that proteins present in the serum (e.g., albumin) may significantly hydrolyze chromogenic substrates such as nitrocefin. Consequently, the LoaD would need to be complemented with an initial step that removes these serum proteins. The third shortcoming is that the measurement accuracy directly relies on the accurate pipetting of sample and reagent volumes in a range of a few μL.

This work reports the design and characterization of a novel point-of-care instrument that can automatically measure the free concentration of the β-lactam piperacillin in 16 μL of diluted serum sample, in a range $[2, 50]$ mg/L relevant to TDM. The method of Brans et al. [11] is adapted to involve a reporter substrate that releases a fluorescent compound upon β-lactamase. The subsequent detection is much more sensitive than absorbance, so it allows to reach the TDM range with a microfluidic LoaD. Moreover, it is insensitive to the presence of proteins in the serum, so prior ultra-filtration of the serum becomes unnecessary. The instrument integrates all the electromechanical components (including robotic pipettes) to handle the fluids automatically within a cube of side length smaller than 50 cm, which is compatible with measurements in space-limited hospital settings. The microfluidic workflow of the LoaD is carefully designed to accurately and robustly select and mix microliter volumes of samples and reagents. The levels of automation and miniaturization reached in this work pave the way to affordable and practical TDM at bedside.

2 Materials and methods

2.1 Reagents

The samples to analyze were made of serum (1:10 diluted human plasma, EFS France) with a different concentration of piperacillin (Viatris, India). The enzyme BlaP99 was prepared at concentration 1.3 nM [19]. A fluorogenic reporter substrate denoted CC1 was synthesized. This substrate was based on a cephalosporin β-lactam, for which the 3' position of cephalosporin was linked to the 7-hydroxy group of an umbelliferone fluorophore [10]. Upon β-lactamase activity on CC1, the β-lactam ring is cleaved, triggering the spontaneous release of the umbelliferone (Figure 1). CC1 was synthesized in three steps, starting from GCLE, according to methods described in Gao et al. [20]. Additionally, a coumarin derivative was synthesized in two steps, starting from

umbelliferone to enable its coupling with intermediate 4-methoxybenzyl (6R,7R)-3-((iodotriphenyl-l5-phosphaneyl)methyl)-8-oxo-7-(2-phenylacetamido)-5-thia-1-azabicyclo[4.2.0]oct-2-ene-2-carboxylate to obtain CC1. The substrate was prepared at 400μM in PBS (KH_2PO_4 1.76 mM, $Na_2HPO_4 \cdot 2H_2O$ 10 mM, NaCl, 137 mM, KCl 2.7 mM buffer pH 7.4, all chemicals form Sigma-Aldrich).

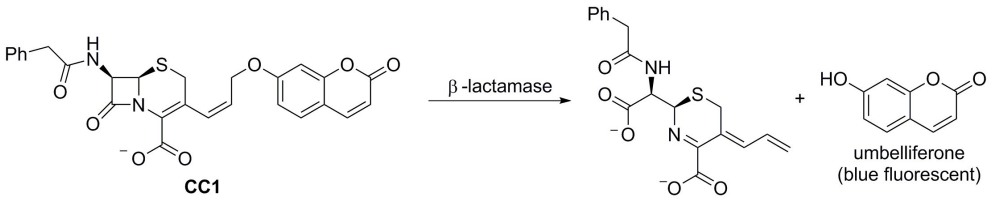

Fig. 1 Release of fluorescent umbelliferone upon β-lactamase cleavage of the fluorogenic substrate CC1.

2.2 Microfluidic design of the LoaD

An unknown antibiotic concentration a in a serum sample can be determined from three other samples with known concentrations: in this work, $a_1 = 0$ mg/L (control), $a_2 = 2$ mg/L (lower bound), and $a_3 = 50$ mg/L (upper bound). The LoaD should perform the enzymatic assay on these four samples simultaneously in the most similar conditions, so the unknown concentration can be inferred from a comparison of the four corresponding fluorescent signals. Therefore, the LoaD contained four identical microfluidic modules (one per antibiotic concentration), in which the same microfluidic workflow had to be performed simultaneously. This workflow comprised four steps, illustrated by four levels in the microfluidic design of Figure 2:

(1) The three reagents (enzyme, serum sample with possibly antibiotic, and fluorogenic substrate) were pipetted in inlet microfluidic chambers.
(2) The LoaD was set in rotation, and each liquid plug was transferred to a metering chamber where an aliquot of precise volume was selected thanks to an overflow mechanism.
(3) The three aliquots of each module were transferred to a mixing chamber where they were merged to initiate the reactions.
(4) The mixture was transferred to a storage chamber where fluorescence intensity was measured to record the progress of the substrate hydrolysis by BlaP99 β-lactamase.

The liquid plugs had to be prevented from reaching the metering chambers during the dispensing step (1), as proper metering was only achieved once the LoaD was rotated. Moreover, the plugs had to be released synchronously from the metering chambers into the mixing chamber, to ensure that the four reactions started releasing the fluorescent umbelliferone at the very same time.

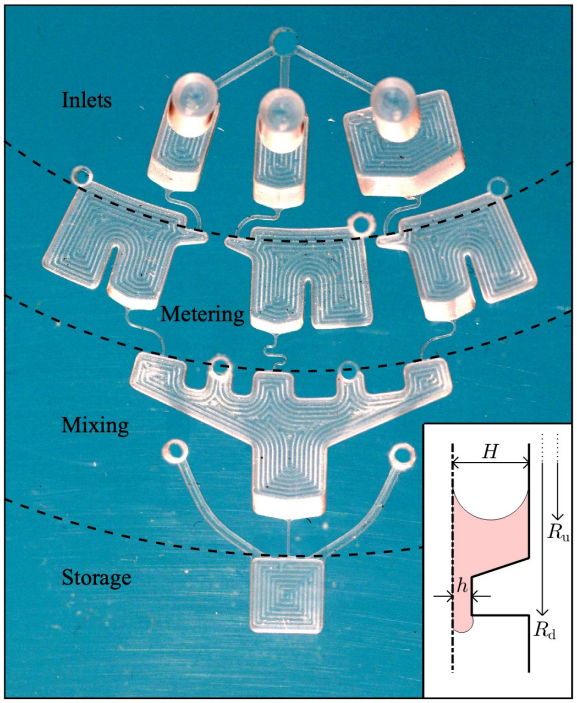

Fig. 2 Top-view of one of the four modules present in the LoaD. The microfluidic network comprised, from the most radially inward to the most radially outward: three inlet chambers (enzyme, serum, and reporter substrate, from left to right), three metering chambers (with adjacent waste chambers), one mixing chamber, and one storage chamber. The chambers were linked by narrow channels. The vents were through-holes in the disk. The scale can be deduced from the width of the storage chamber, which was 4 mm. The three dashed arcs are virtual lines indicating the radial position of capillary burst valves. (Inset) Schematic zoomed cross-sectional view of a capillary burst valve. The thick solid line is the PMMA disk while the dash-dotted line is the covering tape. The liquid plug, shaded in red, extends from radial position R_u in the upstream chamber (interface curvature $\sim 2/H + 2/W$) to the valve at radial position R_d (interface curvature $\sim 2\alpha/h$).

Synchronization was achieved by operating capillary burst valves located at the exit of the channels bringing fluids to the metering chambers (onset of step 2) and to the mixing chamber (onset of step 3). These valves are based on the competition of centrifugal and capillary forces. In a microfluidic network where each chamber is vented, fluid plugs move outward provided that the centrifugal pressure differential Δp_c along them overcomes the sum of Laplace pressure jumps Δp_u and Δp_d across upstream and downstream interfaces. To cross the abrupt section enlargement from a channel to a chamber, the downstream interface must become strongly curved, in the convex direction if the chamber walls are globally hydrophobic. The corresponding increase in Δp_d opposes further motion of the plug, until Δp_c is increased to the same level. The centrifugal pressure is evaluated as $\Delta p_\mathrm{c} = \rho\Omega^2(R_\mathrm{d}^2 - R_\mathrm{u}^2)/2$, where ρ is the fluid density, R_u and R_d are the radial positions of upstream and downstream plug

interfaces respectively (Figure 2 - inset), and Ω is the angular velocity of the LoaD. For a downstream interface at the exit of a square channel of width h, the Laplace pressure jump is $\Delta p_{\mathrm{d}} = 2\alpha\sigma/h$, where σ is the surface tension of the fluid and α is a dimensionless factor of the order unity that depends on the advancing contact angle on each wall. Similarly, for an upstream interface in a rectangular chamber of width W and depth H with receding contact angles close to 0, the Laplace pressure jump is approximately $\Delta p_{\mathrm{u}} = 2\sigma(1/H + 1/W)$. In each case, we chose $10h \leq H < W$, so $\Delta p_{\mathrm{d}} \gg \Delta p_{\mathrm{u}}$ and the channel exits were always the main obstacles to plug motion. The opening of capillary burst valves was controllably triggered by increasing Ω until $\Delta p_{\mathrm{c}} > \Delta p_{\mathrm{d}}$. The factor $\alpha = 1.25$ was determined empirically by measuring the critical speed Ω at which each valve opens. Importantly, the uncertainty on this factor was about 15%, so a safety factor of +/- 20% had to be considered in the microfluidic design.

The design of one module is shown in Fig. 2. All the chambers were vented with additional holes, except the inlet chambers where the inlet holes were sufficiently large to provide venting. The latter were designed to receive 16μL of enzyme, 16μL of serum, and 32μL of fluorogenic substrate. The width of the metering chambers was $W_2 = 2.9$ mm. Their depth was $H_2 = 1$ mm for both enzyme and serum, and $H_2 = 2$ mm for the substrate, yielding selected volumes of the order of 9 μL and 18 μL, respectively. Waste chambers were placed adjacent to the metering chambers to collect the non-selected liquid volume overflowing from the metering chambers.

Microchannels with a squared cross-section connected each inlet chambers to the corresponding metering chamber, and each metering chamber to the mixing chamber. The volume of these channels was less than 0.6 μL, i.e., much smaller than the plug volumes. The exit of each channel acted as a capillary burst valve.

Once all these valves opened, the plugs merged in the mixing chamber and were then progressively transferred to the storage chamber downstream. The storage capacity of the mixing chambers was 32 μL, i.e., slightly less than the sum of selected liquid volumes, to ensure that they were completely filled. In theory, fluorescence measurements could already be taken in the mixing chambers. However, the measurements had to be done once the LoaD stopped spinning. In earlier designs without a storage chamber, the liquid plug was partially thrown out of the mixing chamber in response to the angular deceleration. The subsequent air bubbles in the mixing chamber significantly altered the measurements. By contrast, once transferred to a slightly undersized storage chamber, the plug marginally shifted through narrow venting channels (depth 0.25 mm, width 0.5 mm), and the storage chamber remained completely filled. While the transition from shallow channels to deep chambers was abrupt on purpose, the reverse transition, from chambers to channels, was smoothed with bevels at an inclination of 60°.

The design (sizing and positioning) of all these microfluidic features is detailed in the supplementary material. The LoaD was machined by milling microfluidic features in a PMMA disk with a diameter of 120 mm and thickness 5 mm. A systematic error of $+20$ μm was observed on chamber width dimensions, and -20 μm on chamber depth dimensions, in addition to a random error of ± 5 μm on every dimension. The

microfluidic network was then closed with a tape (polypropylene film with acrylic-based adhesive coating, 3635E5-38B297 from Labelor).

2.3 Instrument prototype to interface the LoaD

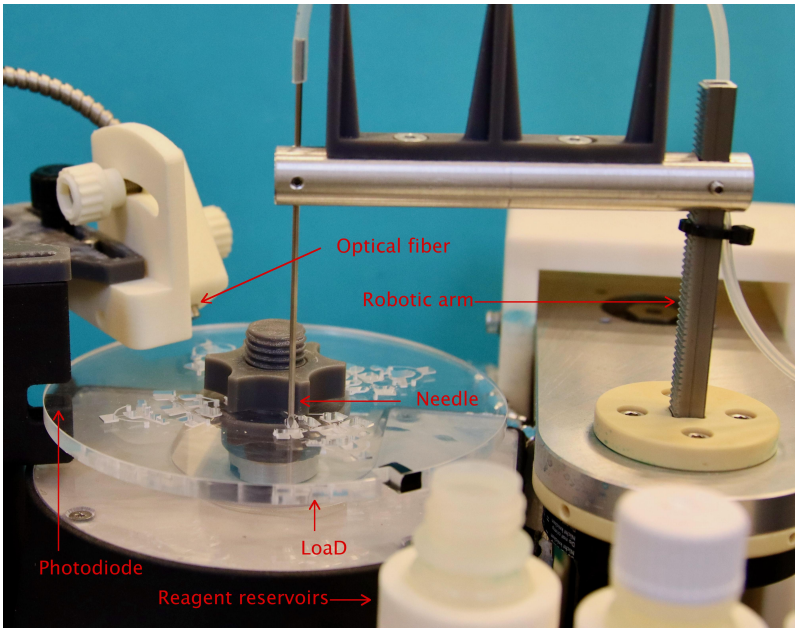

Fig. 3 Inside of the instrument prototype. The LoaD, the photodiode to detect the angular position of the LoaD, the reagent reservoirs, the needle fed by the pipette, the robotic arm, and the optical fiber connected to the spectrophotometer are annotated. Although the picture is a central projection for which there is no unique scale, dimensions can be estimated by comparison to the LoaD diameter, which is 120 mm.

A compact home-made instrument prototype (Fig. 3) was designed and built to interface the LoaD (rotation control and imaging, fluid dispensing, and fluorescence measurement). The rotation was controlled with a stepper motor (PKP566N28A2-R2GL, from Oriental Motor) interfaced with a microcontroller (STM32-F103RBT6, from STmicroelectronics). Once per turn, the controller sent a TTL signal to a camera (S-25A70, from Adimec), which took a picture of the whole LoaD in bright-field conditions. The absolute angular position of the LoaD was determined thanks to a photodiode. The latter was placed to detect the passage of a small square of opaque tape (side 5 mm) glued at the LoaD edge. Once this position was known, it was possible to set the disk at any specific angular position, e.g., during the fluorescence measurements in each chamber. The different reagents were initially stored in bottles or 2 mL Eppendorf tubes in the vicinity of the LoaD. They were pumped out and injected in the inlet chambers of the LoaD thanks to a robotized pipette (Dilutor 401, from Gilson). The needle (SGS Analytical, reference NLL-11.5/14) had a sharp

beveled tip that pierced the tape covering the inlets and dispensed the fluids therein. It was mounted on a robotic arm (Drylin HSQ with D7 driver, from Igus) that performed a vertical translation (to move in and out of the reservoirs and LoaD inlets) and a rotation of vertical axis (to move from the reservoir zone to the LoaD zone). The arm was operated by a microcontroller (Nucleo64-L476RG, from STmicroelectronics). Fluorescence was excited at 385 nm with a LED (HPLED-385, from Advantes) and a high-pass filter (400 nm, from Techspec). The intensity of emitted light was measured at 455.3 nm thanks to a spectrophotometer (AvaSpec-ULS2048x64-EVO, from Advantes) and a low-pass filter (GL-GG395-12, from Schott). An optical fiber (FC-UVIR600-1-BX, from Advantes) transmitted light back and forth to the LoaD. Its tip was positioned at 10 mm from the storage chambers and inclined at 45°. The LoaD and its motor, the robotic arm and the reservoirs were enclosed in a thermostatic chamber at 37 °C. The total dimensions of the prototype are 38 cm (length), 28 cm (width) and 42 cm (height). Although these dimensions can be further reduced with an optimization of component positioning, they are already in a range compatible with the demanding space requirements of intensive care units.

2.4 Workflow

Once the pipette and robotic arm had dispensed each reagent in the corresponding inlet chamber of the LoaD, the latter was rotated according to the following sequence of steps, with an angular acceleration of 5000 rpm/s at every change of rotation speed:

(1) The rotational speed was set at $\Omega_1 = 550$ rpm for 6 s, which brought the liquid plugs at the valves downstream of the inlet chambers.
(2) The rotational speed was increased to $\Omega_p = 1050$ rpm for 0.1 s to open these valves. Then it was reduced to $\Omega_2 = 650$ rpm for 20 s, and the liquid plugs were transferred to the metering chambers where defined volumes were selected.
(3) The rotational speed was increased to $\Omega_3 = 2500$ rpm for 4 s. The second set of capillary valves opened and all the liquids were successively transferred to the mixing and to the storage chambers. The LoaD was then gently brought back to rest (deceleration at 1250 rpm/s).
(4) Finally, the LoaD was slowly moved to successively align each of the four storage chambers with the optical fiber. Fluorescence was recorded in each chamber every 5 s for 60 s.

This sequence is justified by the design calculations available in supplementary material.

2.5 Measurements in well plates

In order to confirm the LoaD results, the kinetic parameters of BlaP99 β-lactamase with the fluorogenic substrate CC1 were independently measured in conventional 96-well plates (Greiner Bio Lab, Belgium), thanks to a thermostatized Tecan Infinite 200 Pro spectrophotometer set at 37°C.

Excitation and emission wavelengths for umbelliferone were 380 nm and 460 nm, respectively [21]. The final reaction volume was always 210 μL, at pH 7.5. The molar fluorescence coefficient (conversion factor from fluorescence units to umbelliferone concentration) was inferred by measuring fluorescence simultaneously for a solution of umbelliferone at concentration of 100 μM (7383 fluorescence units) and for a solution without umbelliferone (background, at 360 fluorescence units). All the kinetic measurements were taken with an identical spectrophotometer configuration.

For the determination of K_m and k_cat, the substrate concentration s_0 was varied from 1 μM to 100 μM while there were no piperacillin ($a_0 = 0$). For the determination of K'_m, the piperacillin concentration a_i (before mixture) was varied from 0 mg/L to 100 mg/L. Volumes and concentrations of each reagent for all these measurements are available in the supplementary material.

3 Results and discussion

3.1 Microfluidic sequence

Snapshots taken during one sequence of LoaD rotation are shown in Figure 4. In Fig. 4(a), reagents had just been dispensed in the inlet chambers, but the rotation had not started yet, so the fluid interfaces were only shaped by gravity and capillary forces.

Fig. 4(b) corresponds to the end of step (1). The centrifugal force pushed the reagents at the most radially outward position of the inlet chambers, and they invaded the channels leading to the metering chambers, but they were stopped at the first capillary valves.

Step (2) started with a very short pulse of high rotation speed, which aim was to burst the valves at the entrance of the metering chambers while leaving the valves at the entrance of the mixing chamber closed. This pulse strategy, first proposed by Kinahan et al. [22], is very effective for sequentially bursting capillary valves in series. Figure 4(c) shows the LoaD right after the pulse. Both the enzyme and the serum crept along the wall of their metering chamber and invaded the subsequent channel to the mixing chamber. At that time, the substrate was still in the nose-shaped part at the top of its metering chamber. This difference in flow speed between the reagents may have resulted from a difference of interface level in the inlet chambers, a different nose depth, a difference of physical properties (mostly viscosity, surface tension and contact angles) or a slight difference of channel size due to imperfect microfabrication. For this reason, the total duration of step (2) in the sequence was chosen to 20 s. It was significantly longer than the normal time for the fluids to transfer in the metering and waste chambers. Therefore, it guaranteed that fluid interfaces in these chambers had reached equilibrium and that the volume selection of each reagent was accurate once the valves to the mixing chamber opened. The nose-shaped design was aimed at forcing the liquids to creep along the chamber walls. Without this nose, liquids sometimes formed detached jets beyond the capillary valve. These jets induced variations of flow rate and sometimes a closure of the capillary valve. The transition from creeping to jetting appeared unpredictable, which may be explained given the relatively low rotation speed of $\Omega_2 = 650$ rpm. Indeed, at the neck of the metering chamber (radial position $r_\mathrm{n} = 29$ mm), the centrifugal acceleration was only $a_\mathrm{c} = r_\mathrm{n}\Omega^2 = 134\mathrm{m/s}^2$,

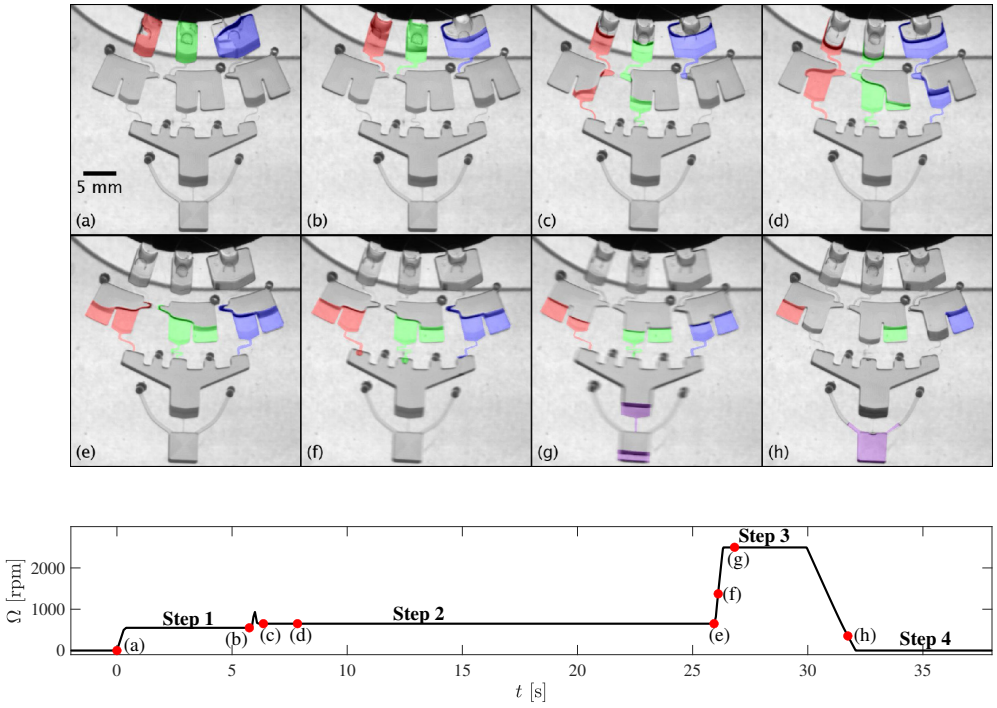

Fig. 4 Snapshots of one module of the LoaD during the execution of the rotation sequence. The liquid plugs have been colored by image processing for the sake of clarity: (red) enzyme BlaP99, (green) serum with piperacillin, (blue) substrate CC1, (purple) mixture of the three reagents. (a) Initial time $t = 0$ s. (b) End of step 1 at $t = 5.75$ s. (c) Start of step 2 at $t = 6.36$ s. (d) Step 2 at $t = 7.84$ s. (e) End of step 2 at $t = 25.93$ s. (f) Start of step 3 at $t = 26.11$ s. (g) Step 3 at $t = 26.82$ s. (h) End of step 3 at $t = 31.74$ s. The graph represents the rotation speed Ω of the LoaD vs. time t. The red dots correspond to the times of the eight snapshots.

which corresponded to an effective capillary length of $\sqrt{\sigma/(\rho a_c)} = 0.7$ mm. As the chamber depth was similar, capillary forces played a significant role in shaping fluids. They would have decided whether fluids crept or formed jets if geometrical artifacts such as the nose had not been added.

In Fig. 4(d), still during step (2), the three pairs of chambers were at different levels of completion of metering. In the middle pair, the metering chamber was full and the serum in excess overflew to the waste chamber. In the right pair, the substrate solution was still filling its metering chamber. In the left pair, the enzyme solution was just about to overflow. It shows that the liquid interface must come significantly higher than the crest separating metering and waste chambers for the overflow to occur. This required distance above the crest approximately corresponds to the effective capillary length.

Figure 4(e) shows the very end of step (2), where the liquid interfaces were at equilibrium and the valves downstream remained closed. Figure 4(f) shows the beginning of step (3) a fraction of a second later. At the time of this snapshot, the rotation

speed was already twice higher than in step (2), and the centrifugal pressure was correspondingly four times higher, thereby largely exceeding the pressure to burst the valve.

Snapshot 4(g) shows the liquids arriving in the mixing and storage chambers. The capillary valve at the end of the channel to the storage chamber was quickly opened, given the high rotation speed of step (3). A similar experiment was made with different food dyes added to the solution to reveal the mixing in the chambers (Figure 4 in the supplementary material). The mixture was further homogenized by crossing the channel to the storage chamber. It means that within the 4 seconds of step (3), the three reagents were brought together and mixed, which started the enzymatic reaction.

Snapshot 4(h) shows the LoaD once the rotation was stopped at the end of step (3). The liquid had slightly invaded the two symmetrical channels that vented the storage chamber. The chamber was full, except for a tiny bubble next to the capillary valve. The influence of this bubble on the fluorescence measurement in the storage chamber was assumed marginal.

3.2 Microfluidic robustness and accuracy

The robustness of the valves was checked by repeating the same sequence 44 times, with the same reagents (except for the piperacillin concentration that was varied), over seven different days. None of the 1056 capillary valves (44 runs x 4 modules x 6 valves per module) failed to control fluid passage according to the expected sequence.

The metered volumes were estimated by multiplying the measured chamber depth by the wet area as seen from snapshots equivalent to Fig. 4(e) in each module and each run of the LoaD. This wet area was obtained by tracking the chamber boundaries and the upstream fluid interface by image processing. This step involved a manual identification of some chamber boundaries. Its repeatability was assessed by measuring 11 times the same wet area. The coefficient of variation was 0.9%. The error corresponding to pixel discretization was 1.7%. The estimated volumes metered in the three chambers were on average 8.93 μL (enzyme), 9.22 μL (serum), and 17.4 μL (substrate). The coefficient of variation was 3%, and variation was equally distributed between different modules and between different runs. Variations from one module to another are possibly explained by the limited precision of micromachining. The volume ultimately in the storage chamber varied between 32 μL (venting channels empty) and 33.5 μL (venting channels almost full). This variation of $\pm$2.3% on the total volume is compatible with the $\pm$3% error on individual metered volumes. However, the sum of these three volumes is on average 2 μL higher than this upper bound on stored liquid volume. This may be explained by the slight transfer between metering and waste chambers that was still observed at the onset of step (3), i.e., between Fig. 4(e) and Fig. 4(f). It may also be explained by a slight lift of the sealing tape in the storage chamber induced by centrifugal pressure.

3.3 Enzymatic assay in the LoaD

Each module was loaded with a different concentration a_i of antibiotic in the serum: 0 mg/L, 2 mg/L, 25 mg/L and 50 mg/L. The intensity of fluorescence I_f measured over

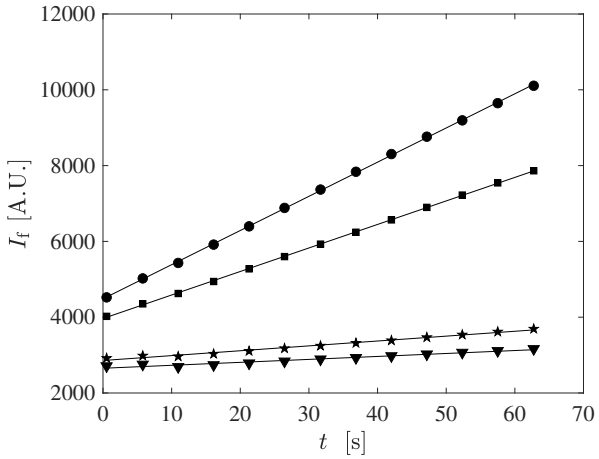

Fig. 5 Fluorescence intensity I_f (arbitrary units) vs. time (s) in the storage chambers of a LoaD. The symbols represent measurements in the four different modules: (▼) $a_i = 50$ mg/L, (★) $a_i = 25$ mg/mL,(■) $a_i = 2$ mg/L, (●) $a_i = 0$ mg/L. The solid lines are linear approximations.

time in each storage chamber is reported in Figure 5. It increased linearly with time, which means that the enzymatic reaction was still far from saturation. The calibration constant γ of Eq. (2) was first calculated for each antibiotic concentration a_i in serum,

$$\gamma = \frac{a_0}{\frac{v_{max}}{v} - 1}, \tag{3}$$

where $a_0 = a_i/4$ since the volume of serum was one fourth of the total volume of the mixture. The geometrical average γ_m of the 24 values of γ obtained for 8 runs with 3 non-zero antibiotic concentrations was $\gamma_m = 1.14$ mg/L. The theoretical estimation through γ_m of the 24 antibiotic concentrations in serum was then compared to their known value in the parity plot of Figure 6. The median, quartiles and min/max of the 8 measurements for each known concentration are reported with box plots. The coefficient of variation of measurements around the parity line is ±19%.

In a real antibiotic measurement, three modules would be dedicated to known antibiotic concentration (no antibiotic, minimum concentration of 2 mg/L, and maximum concentration of 50 mg/L), while the fourth module would contain the unknown concentration (here 25 mg/L). In such case, the unknown concentration a_i would be calculated from γ_m corresponding to the geometrical average of γ measured at 2 mg/L and 50 mg/L, for each run separately. The distribution over 8 runs of the calculated a_i had an average of 28 mg/L (systematic error of 12%) and again a coefficient of variation of 19%. Therefore, once the constant γ is determined for an assay, unknown antibiotic concentrations in the range from 2 to 50 mg/L can be measured with an accuracy of 19%.

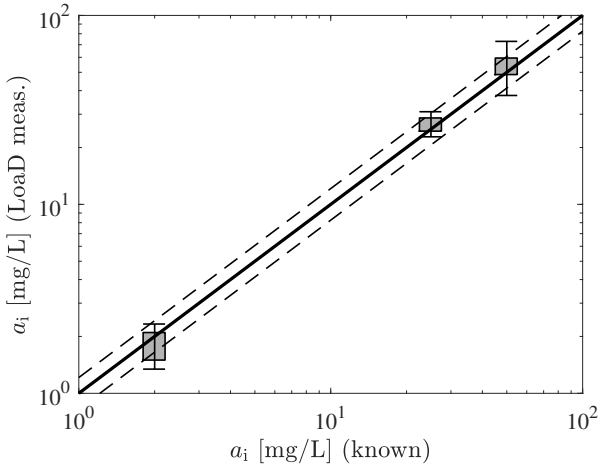

Fig. 6 Parity plot of the measured concentration a_i (inferred from fluorescence intensity measurements) vs. the known concentration a_i of piperacillin in the initial serum. The box plots correspond to the median, interquartile, and minimum/maximum of measured concentration over the 8 runs per known concentration. The solid line is the parity line, while the dashed lines correspond to parity ±19%.

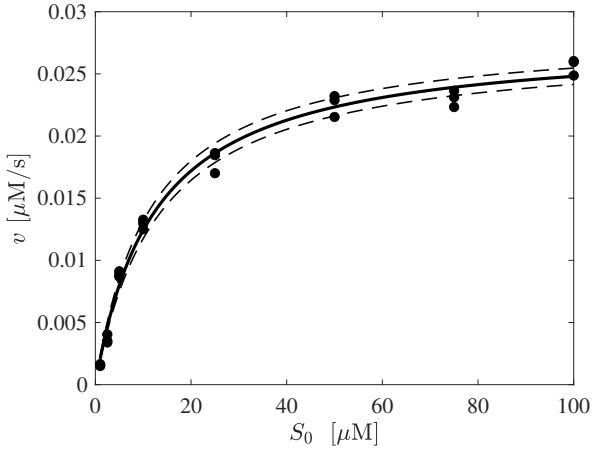

Fig. 7 Production rate v of fluorescent umbelliferone from reporter substrate CC1 through β-lactamase (BlaP99) in the absence of piperacillin. The CC1 concentration s_0 was varied from 1 to 100 μM, while the enzyme concentration was $e_0 = 0.031$ nM. The data points correspond to measurements of fluorescence in a 96 well-plate with a Tecan spectrophotometer (triplicate for each concentration). The solid line represents the least-square fit of eq. (1), with $K_\mathrm{m} = 12.4$ μM and $k_\mathrm{cat} = 907$ s^{-1}. The dashed lines represent the same equation, with ±7% on K_m and ±2% on k_cat.

3.3.1 Comparison with enzymatic assay in well plates

The concentration of umbelliferone produced by the enzymatic reaction was calculated from the fluorescence intensity measurements. The growth rate v of this concentration is constant as long as it remains much smaller than the initial substrate concentration

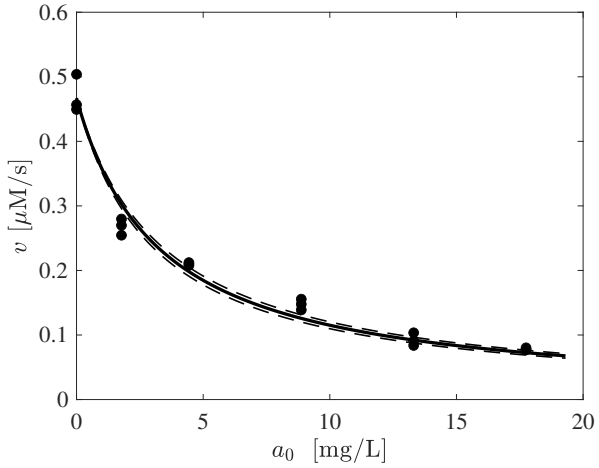

Fig. 8 Production rate v of fluorescent umbelliferone from reporter substrate CC1 through β-lactamase (BlaP99) under inhibition by piperacillin at concentration a_i (before mixture) ranging from 0 to 100 mg/L. The CC1 concentration s_0 was at 171 μM and the enzyme concentration was $e_0 = 0.55$ nM. The data points correspond to measurements of fluorescence in a 96 well-plate with a Tecan spectrophotometer (triplicate for each concentration). The solid line represents the least-square fit of eq. (1), with $K'_\mathrm{m} = 0.115$ μM (parameters K_m and k_cat were fixed at the values determined in Fig. 7). The dashed lines represent the same equation, with $\pm 6\%$ on K'_m.

s_0. The rate v was then determined by fitting umbelliferone concentrations less than 0.2 s_0 with a linear function of time.

Figure 7 shows v for different initial substrate concentrations s_0, in the absence of piperacillin ($a_0 = 0$) and with an enzyme concentration $e_0 = 0.031$ nM. The kinetic parameters inferred by least-square fitting equation 1 on the data of Fig. 7 are $K_\mathrm{m} = 12.4$ μM ($\pm 7\%$) and $k_\mathrm{cat} = 907$ s^{-1} ($\pm 2\%$), with a coefficient of determination $R^2 = 0.99$. Similarly, figure 8 shows v for different piperacillin concentrations a_0, with fixed concentrations of CC1 ($s_0 = 171$ μM) and enzyme ($e_0 = 0.55$ nM). The least-square fit of equation 1 on the data of Fig. 8 allows the determination of $K'_\mathrm{m} = 0.115$ μM ($\pm 6\%$), with a coefficient of determination $R^2 = 0.98$.

By comparison, the parameters measured by Galleni et al. [23] for the hydrolysis of the chromogenic substrate nitrocefin by BlaP99 were $K_\mathrm{m} = 25 \pm 2$ μM and $k_\mathrm{cat} = 780 \pm 30$ s^{-1}. The fact that parameters for CC1 and for nitrocefin are in the same range suggests that CC1 is as adapted as nitrocefin to report a decrease of apparent enzymatic activity upon concentrations of piperacillin in the TDM range. Nevertheless, by contrast to nitrocefin, CC1 is not significantly hydrolyzed by serum proteins (Data in supplementary material, section 1.4), which considerably simplifies pre-analytical processing. The Michaelis constant $K'_\mathrm{m} \simeq 0.115$ μM is 55 times smaller than the value reported in Bush and Sykes [24]. However, it is of the same order of magnitude as the Michaelis constant 0.17 μM reported in Power et al. [25] for the interaction of piperacillin with a similar β-lactamase AmpC M29 from *Morganella morganii* strain PP29. The calibration constant of Eq. (2) is calculated as $\gamma \simeq 0.88$ ($\pm 13\%$), from the kinetic parameters determined in section 3.3.1. It is 23% smaller than the γ determined from LoaD measurements.

The limit of detection (LOD) of the BlaP99 method was experimentally determined for the chromogenic reporter substrate nitrocefin (Supplementary Material, section 4). The LOD was calculated from replicate blank samples according to regulatory guidelines and was established at 1 mg/L. Figures 5 to 8 suggest that this detection limit is also applicable to the fluorogenic reporter substrate CC1.

3.3.2 Sources of error

Equation 2 is only valid in the stationary regime where the concentrations of complexes and acyl-enzyme adducts remain constant. This hypothesis is verified since the timescale $t_\mathrm{m} \in [5, 60]$ s of the measurements is much larger than both $1/k_\mathrm{cat} \sim 1$ ms and $1/k'_\mathrm{cat} \sim 1$ s [24]. Moreover, as shown in the supplementary material, both substrate and antibiotic concentrations remain approximately constant during the measurement. Indeed, the substrate concentration only decreases by at most 9% over t_m, while the antibiotic concentration decreases by less than 1%. This is further confirmed in Fig. 5 by the linear increase with time of the concentration of fluorescent product.

There are several potential sources of error that, together, likely explain the observed variations of the order of 20% and discrepancies between LoaD and well-plate measurements. As demonstrated in the Supplementary Material, the uncertainty of 3% on the metered volume of each reagent accounts for a relative error of 4.2% on the measured production rate v. Although the LoaD and the reagents were in a thermostatic chamber, their temperature may also slightly fluctuate from one run to the next, which modifies the catalytic rate constant k_cat of BlaP99. Considering the Arrhenius law with an activation energy $E_\mathrm{a} \simeq 40$ kJ/mol/K for BlaP99 with β-lactamase [26], a temperature variation of 1 K induces a 5%-variation of both k_cat and v. The enzyme used in the 8 runs of the LoaD originated from two batches that, possibly, slightly differed in terms of enzyme concentration. However, no significant difference was observed between them in terms of γ. The enzyme activity might also decrease from one run to the next, but no significant drift in γ was observed between the first and the last run with each batch. Other sources of error might include an imperfect positioning of the LoaD with respect to the optical fiber through which fluorescence is measured, or an imperfect mixing in the storage chamber.

In the context of POC assays, calibration and measurement would be performed simultaneously on the same LoaD. This approach would help compensate for temperature variations as well as discrepancies between different LoaDs, highlighting the advantage of conducting these measurements in parallel.

Conclusions

There is a significant body of literature indicating a real need for Point-of-Care (PoC) systems that allow for frequent and easy measurement of free antibiotic concentration in serum, particularly for the Therapeutic Drug Monitoring (TDM) of intensive care patients with unpredictable PK/PD parameters. In this work, we developed a Lab on a Disk (LoaD) and associated instrument to perform such measurement automatically. We illustrated its working principle with the concentration measurement of

piperacillin. This β-lactam is set in competition with a fluorogenic reporter substrate to interact with the enzyme BlaP99. The use of a fluorogenic reporter substrate further enhances the LoaD platform by eliminating the ultrafiltration step required for chromogenic assays. Fluorescence can be measured from a single side of the disk, and the signal can be more easily amplified, improving sensitivity. Together with minimal serum preparation, these features facilitate rapid, point-of-care therapeutic drug monitoring in clinical settings. We demonstrated that the kinetic parameters are such that the production rate of this fluorescent compound decreases significantly when the antibiotic concentration increases in a range $[2, 50]$ mg/L relevant to TDM. The corresponding variations of fluorescence intensity are measurable, even in a microfluidic format, and they correlate very well with the variations of antibiotic concentration.

The LoaD designed in this work is based on centrifugal microfluidics. The disk comprises metering chambers to ensure an automated and accurate volume selection of each sample and reagent. The flows are robustly controlled thanks to capillary valves that burst upon pulses in rotation speed of the LoaD. While these valves were often considered non-robust [16], we managed to identify a geometrical design and kinematic parameters that ensure their systematic opening on-demand. With such miniaturization and automation, the LoaD needs only 3 minutes and 16 μL of human serum diluted 10x (i.e., 1.6 μL of non-diluted serum) to provide reproducible measurements of clinically meaningful antibiotic concentrations. This low blood volume requirement is compatible with pediatric use, for which blood sampling must be kept as minimal as possible. Another module can be added to the LoaD to extract either plasma or serum from a whole blood sample [27, 28], thereby providing an antibiotic measurement with a single manual operation (i.e., loading the whole blood sample in the instrument). Such performance can significantly improve the therapeutic monitoring of β-lactams by providing essential pharmacokinetic information in a rapid, bedside-compatible LoaD format. It would enable healthcare staff in intensive care units to adjust doses and maintain curative drug levels throughout the treatment period. In addition, combining rapid therapeutic drug monitoring with rapid pathogen susceptibility assessment (e.g., MIC determination) [29, 30] could substantially improve the management of bacterial resistance.

Supplementary information. The supplementary material comprises:

1. a document, *Medicare-SupplMat.pdf*, that provides calculation notes on (a) the Michaelis-Menten kinetics and associated assumptions, (b) details on the microfluidic design, and (c) details on the validation of the enzymatic assay with a chromogenic substrate.
2. a spreadsheet, *KineticsAllData.xlsx*, that contains all the fluorescence measurements, in the LoaD and with the Tecan spectrophotometer (well-plates).
3. a spreadsheet, *ChamberDesign.xlsx*, in which all the microfluidic design calculations are implemented.
4. a video of one run of the LoaD, *ExampleLoaDRun.avi*.

Acknowledgements. This research was founded by the MEDICARE project, convention 1910067, Program Win2Wal 2019/1 Walloon Region granted to Prof. Bernard

Joris (coordinator). Raphaël Robiette is a Maître de Recherche at F.R.S. - FNRS. The authors thank Denis Vandormael (Sirris) for fruitful discussions and fabrication of the LoaDs, as well as Trystan Gailly for the preliminary characterization of capillary valves.

Declarations

Conflicts of interest: There are no conflicts to declare.
Author contributions: O.V., A.A., R.R., B.J. and T.G. designed the experiments and the methodology. M.R., S.W. and R.R. synthesized the fluorogenic reporter substrates. O.V. developed the LoaD interface and software. O.V., A.A. and T.G. processed the data. A.A., R.R., B.J. and T.G. wrote the manuscript. R.R., B.J. and T.G. supervised the work.

References

[1] Bush, K., Bradford, P.A.: β-lactams and β-lactamase inhibitors: An overview. Cold Spring Harbor Perspect. Med. **6(8)**, 025247 (2016) https://doi.org/10.1101/cshperspect.a025247

[2] Tilanus, A., Drusano, G.: Optimizing the use of beta-lactam antibiotics in clinical practice: A test of time. Open Forum Infect. Dis. **10(7)**, 305 (2023) https://doi.org/10.1093/ofid/ofad305

[3] Wong, G., Briscoe, S., Adnan, S., McWhinney, B., Ungerer, J., Lipman, J., Roberts, J.A.: Protein binding of β-lactam antibiotics in critically ill patients: Can we successfully predict unbound concentrations? Antimicrob. Agents Chemother. **57**(12), 6165–6170 (2013) https://doi.org/10.1128/aac.00951-13

[4] Abdul-Aziz, M.H., Brady, K.M., Cotta, M.O., Roberts, J.A.: Therapeutic drug monitoring of antibiotics: Defining the therapeutic range. Ther. Drug Monit. **44(1)**, 19–31 (2022) https://doi.org/10.1097/FTD.0000000000000940

[5] Abdul-Aziz, M.H., Hammond, N.E., Brett, S.J., Cotta, M.O., De Waele, J.J., Devaux, A., Di Tanna, G.L., Dulhunty, J.M., Elkady, H., Eriksson, L., Hasan, M.S., Khan, A.B., Lipman, J., Liu, X., Monti, G., Myburgh, J., Novy, E., Omar, S., Rajbhandari, D., Roger, C., Sjövall, F., Zaghi, I., Zangrillo, A., Delaney, A., Roberts, J.A.: Prolonged vs intermittent infusions of β-lactam antibiotics in adults with sepsis or septic shock: A systematic review and meta-analysis. JAMA **332(8)**, 638–649 (2024) https://doi.org/10.1001/jama.2024.9803

[6] Wicha, S.G., Märtson, A.G., Nielsen, E.I., Koch, B.C.P., Friberg, L.E., Alffenaar, J.W., Minichmayr, I.K.: International society of anti-infective pharmacology (isap), the pk/pd study group of the european society of clinical microbiology, infectious diseases (epasg). from therapeutic drug monitoring to model-informed

precision dosing for antibiotics. Clin. Pharmacol. Ther. **109(4)**, 928–941 (2021) https://doi.org/10.1002/cpt.2202.7

[7] Abdul-Aziz, M.H., Alffenaar, J.C., Bassetti, M., Bracht, H., Dimopoulos, G., Marriott, D., Neely, M.N., Paiva, J.A., Pea, F., Sjovall, F., Timsit, J.F., Udy, A.A., Wicha, S.G., Zeitlinger, M., De Waele, J.J., Roberts, J.A.: Infection section of european society of intensive care medicine (esicm); pharmacokinetic/pharmacodynamic and critically ill patient study groups of european society of clinical microbiology and infectious diseases (escmid); infectious diseases group of international asso-ciation of therapeutic drug monitoring and clinical toxicology (iatdmct); infections in the icu and sepsis working group of international society of antimicrobial chemotherapy (isac). antimicrobial therapeutic drug monitoring in critically ill adult patients: a position paper. Intensive Care Med. **46(6)**, 1127–1153 (2020) https://doi.org/10.1007/s00134-020-06050-1

[8] Dhaese, S., Van Vooren, S., Boelens, J., De Waele, J.: Therapeutic drug monitoring of β-lactam antibiotics in the icu. Expert Rev. Anti-infect. Ther. **18**(11), 1155–1164 (2020) https://doi.org/10.1080/14787210.2020.1788387

[9] Roberts, J.A., Abdul-Aziz, M.H., Lipman, J., Mouton, J.W., Vinks, A.A., Felton, T.W., Hope, W.W., Farkas, A., Neely, M.N., Schentag, J.J., Drusano, G., Frey, O.R., Theuretzbacher, U., Kuti, J.L.: International society of anti-infective pharmacology and the pharmacokinetics and pharmacodynamics study group of the european society of clinical microbiology and infectious diseases. individualized antibiotic dosing for patients who are critically ill: challenges and potential solutions. Lancet Infect Dis. **14(6)**, 498–509 (2014) https://doi.org/10.1016/S1473-3099(14)70036-2

[10] Mabilat, C., Gros, M.F., Nicolau, D., Mouton, J.W., Textoris, J., Roberts, J.A., Cotta, M.O., Belkum, A., Caniaux, I.: Diagnostic and medical needs for therapeutic drug monitoring of antibiotics. Eur. J. Clin. Microbiol. Infect. Dis. **39(5)**, 791–797 (2020) https://doi.org/10.1007/s10096-019-03769-8

[11] Brans, A., Joris, B., Delmarcelle, M., Marchand, J., Hammaecher, C., Tulkens, P., Goormaghtigh, E., De Coninck, J.: Enzymatic Method for Rapid and Continuous Determination of Beta-lactamic Antibiotics. WO2013053953, WO2013053953

[12] Joris, B., Amoroso, A., Verlaine, O.: Methods for Determining the Concentration of a Carbapenem Antibiotic in a Biological Sample. EP3997240, EP3997240

[13] Ducrée, J., Haeberle, S., Lutz, S., Pausch, S., Stetten, F., Zengerle, R.: The centrifugal microfluidic bio-disk platform. J. Micromech. Microeng. **17**, 103–115 (2007) https://doi.org/10.1088/0960-1317/17/7/S07

[14] Gorkin, R., Park, J., Siegrist, J., Amasia, M., Lee, B.S., Park, J.M., Kim, J., Kim, H., Madou, M., Cho, Y.K.: Centrifugal microfluidics for biomedical applications. Lab Chip **10(14)**, 1758–1773 (2010) https://doi.org/10.1039/b924109d

[15] Strohmeier, O., Keller, M., Schwemmer, F., Zehnle, S., Mark, D., Stetten, F., Zengerle, R., Paust, N.: Centrifugal microfluidic platforms: advanced unit operations and applications. Chem. Soc. Rev. **44(17)**, 6187–6229 (2015) https://doi.org/10.1039/c4cs00371c

[16] Peshin, S., Madou, M., Kulinsky, L.: Microvalves for applications in centrifugal microfluidics. Sensors **22(22)**, 8955 (2022) https://doi.org/10.3390/s22228955

[17] Gholizadeh, A., Mazzucchelli, G., Gilet, T.: Flipping: A valve-free strategy to control fluid flow in centrifugal microfluidic systems. Sens. Actuators B-Chem. **412**, 135778 (2024) https://doi.org/10.1016/j.snb.2024.135778

[18] Duffy, D.C., Gillis, H.L., Lin, J., Sheppard, N.F., Kellogg, G.J.: Microfabricated centrifugal microfluidic systems: characterization and multiple enzymatic assays. Anal. Chem. **71(20)**, 4669–4678 (1999) https://doi.org/10.1021/ac990682c

[19] Wouters, J., Charlier, P., Monnaie, D., Frère, J.M., Fonzé, E.: Expression, purification, crystallization and preliminary x-ray analysis of the native class c beta-lactamase from enterobacter cloacae 908r and two mutants. Acta Crystallogr. D **57(1)**, 162–164 (2001) https://doi.org/10.1107/s0907444900016413

[20] Gao, W., Xing, B., Tsien, R.Y., Rao, J.: Novel fluorogenic substrates for imaging beta-lactamase gene expression. J. Am. Chem. Soc. **125(37)**, 11146–11147 (2003) https://doi.org/10.1021/ja036126o

[21] Berkel, S.S., Brem, J., Rydzik, A.M., Salimraj, R., Cain, R., Verma, A., Owens, R.J., Fishwick, C.W.G., Spencer, J., Schofield, C.J.: Assay platform for clinically relevant metallo-β-lactamases. J. Med. Chem. **56**(17), 6945–6953 (2013) https://doi.org/10.1021/jm400769b

[22] Kinahan, D.J., McConville, K., Henderson, B., McCaul, M., McNamara, E., Diamond, D., Ducrée, J.: Digital pulse actuated flow control on a centrifugal disc towards multiparameter water quality monitoring. In: 20th International Conference on Miniaturized Systems for Chemistry and Life Sciences (2016)

[23] Galleni, M., Lindberg, F., Normark, S., Cole, S., Honoré, N., Joris, B., Frère, J.-M.: Sequence and comparative analysis of three *enterobacter cloacae* ampc β-lactamase genes and their products. Biochem. J. **250**, 753–760 (1988)

[24] Bush, K., Sykes, R.B.: Methodology for the study of β-lactamases. Antimicrob. Agents Chemother. **30 (1)**, 6–10 (1986) https://doi.org/10.1128/aac.30.1.6

[25] Power, P., Galleni, M., Ayala, J.A., Gutkind, G.: Biochemical and molecular characterization of three new variants of ampc β-lactamases from *morganella morganii*. Antimicrob. Agents Chemother. **50 (3)**, 962–967 (2006) https://doi.org/10.1128/aac.50.3.962-967.2006

[26] Cartwright, S.J., Waley, S.G.: Cryoenzymology of beta-lactamases. Biochemistry **26(17)**, 5329–5337 (1987) https://doi.org/10.1021/bi00391a017

[27] Haeberle, S., Brenner, T., Zengerle, R., Ducrée, J.: Centrifugal extraction of plasma from whole blood on a rotating disk. Lab Chip **6**, 776–781 (2006) https://doi.org/10.1039/b604145k

[28] Kuo, J.-N., Li, B.-S.: Lab-on-cd microfluidic platform for rapid separation and mixing of plasma from whole blood. Biomed. Microdevices **16**, 549–558 (2014) https://doi.org/10.1007/s10544-014-9857-1

[29] Wu, W., Zhao, Q., Cai, G., Zhang, B., Suo, Y., Liu, Y., Jin, W., Mu, Y.: All-in-one escherichia coli viability assay for multi-dimensional detection of uncomplicated urinary tract infections. Anal. Chem. **94**(51), 17853–17860 (2022) https://doi.org/10.1021/acs.analchem.2c03604

[30] Wu, W., Cai, G., Liu, Y., Suo, Y., Zhang, B., Jin, W., Yu, Y., Mu, Y.: Direct single-cell antimicrobial susceptibility testing of escherichia coli in urine using a ready-to-use 3d microwell array chip. Lab Chip **23**(10), 2399–2410 (2023) https://doi.org/10.1039/D2LC01095J